ORGANOMETALLICS

pubs.acs.org/Organometallics Article

Investigations of the Reaction of HB(pin) with Tris(amido) Y(III) Complexes

Rana B. Abdu and Courtney C. Roberts*

Cite This: *Organometallics* 2025, 44, 995−999 Read Online

ACCESS Metrics & More | Article Recommendations | Supporting Information

ABSTRACT: Transmetallation, or transfer of a group between metals or metalloids, is arguably the most understudied elementary organometallic step, especially with early transition metal complexes. In this work, the reactivity of the organoborane, HB(pin), with yttrium complexes bearing a tris(amido) redox-active ligand was investigated. B−O bond cleavage was observed instead of the expected B−H bond cleavage that would result from transmetallation. Additionally, the tris(amido) ligand was transferred from yttrium to boron. New boron complexes (**2**) and (**3**) were synthesized and characterized and an intermediate Y−B complex (**4**) featuring the B−O bond cleavage is also reported. This work demonstrates the incompatibility of HB(pin) as a transmetallating reagent for yttrium complexes bearing a tris(amido) ligand.

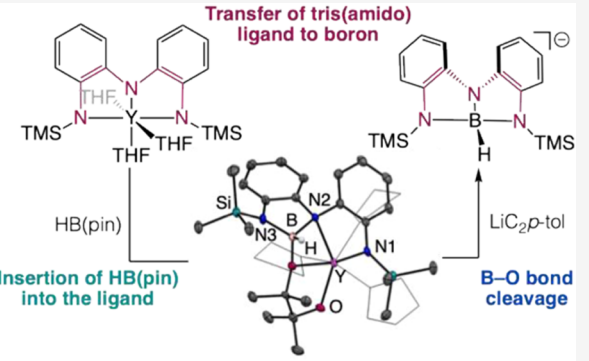

INTRODUCTION

Cross−coupling reactions to form C−C bonds have been widely used in the synthesis of pharmaceuticals and agrochemicals.[1,2] While many cross−coupling reactions are mediated by late transition metal catalysts such as Fe, Co, Ni, Cu, and Pd, our group reported an alkyl−alkyl cross−coupling reaction catalyzed by early transition metal and lanthanide complexes bearing a tris(amido) redox−active ligand.[3−14] This is the first example of a catalytic $C(sp^3)$−$C(sp^3)$ cross−coupling reaction enabled by d^0 metal complexes bearing a redox−active ligand. Due to the novelty of the transformation, we were interested in expanding the utility of this cross−coupling reaction beyond $C(sp^3)$−$C(sp^3)$ by investigating its elementary steps. Specifically, we sought to better understand transmetallation, the transfer of a group from one metal or metalloid to another, as it is the most underexplored elementary organometallic step.

The reactivity of late transition metals with transmetallating reagents such as organolithium compounds, Grignard reagents, organozinc reagents, organostannanes, and organoboranes has been widely explored.[15−26] However, the comparable reactivity of early transition metals has been vastly underexplored. Organoboranes are attractive transmetallating reagents as they are readily available, tend to be less sensitive to air and water, and are less toxic when compared to other commonly used transmetallating reagents. This led us to explore organoboranes as compatible transmetallating reagents with early transition metal complexes (Figure 1a). Pinacolborane, HB(pin), was selected as the transmetallating reagent for this work as the rate of transmetallation is faster the more *s*−character the atom being transferred has.[27] Additionally, the hydride is the least sterically hindered group possible, which would allow for more facile transmetallation.

There is some precedent in the literature for the reactivity of early transition metal complexes with HB(pin). The Chen group reported a scandium phosphinidene complex, a scandium phosphinoalkylidene complex, and a terminal scandium imido complex, all of which performed a B−O bond cleavage of HB(pin) to generate scandium complexes bearing the pinacolato group.[28−30] This piqued our interest, as we wanted to investigate if the B−H bond can be cleaved instead of the B−O bond, resulting in hydride transfer to the early transition metal. We reasoned that less reactive early transition metal complexes would result in B−H bond cleavage of HB(pin) over B−O bond cleavage due to the relative bond strength of B−H bond being weaker. In this work, we investigated the reactivity of HB(pin) with yttrium complexes bearing a tris(amido) redox−active ligand (Figure 1b). Interestingly, we found that B−O bond cleavage is observed instead of B−H bond cleavage even with less reactive early transition metal complexes. In addition, the tris(amido) ligand is transferred from yttrium to boron.

Received: February 20, 2025
Revised: April 4, 2025
Accepted: April 16, 2025
Published: April 22, 2025

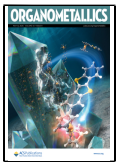

https://doi.org/10.1021/acs.organomet.5c00068
Organometallics 2025, 44, 995−999

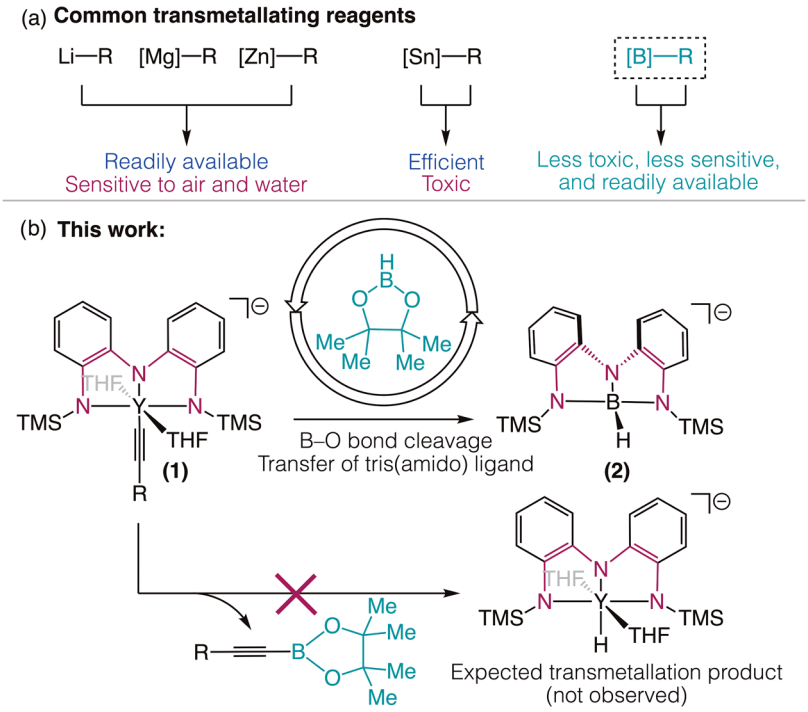

Figure 1. (a) Common transmetallating reagents. (b) Reactivity of HB(pin) with yttrium complexes bearing a tris(amido) ligand.

RESULTS AND DISCUSSION

Synthesis and Characterization of Li(THF)$_2$[(NNN)Y-(C_2*p*-tol)(THF)$_2$] (1). We chose to perform transmetallation studies of HB(pin) with an yttrium acetylide complex, Li(THF)$_2$[(NNN)Y(C_2*p*-tol)(THF)$_2$] (**1**), as cross−coupling of alkynes is of interest to us. Complex (**1**) was synthesized by dissolving a neutral (NNN)Y(THF)$_3$ complex in THF and adding LiC_2*p*-tol at −78 °C (Scheme 1). Complex (**1**) was isolated as a yellow powder in 89% yield, which was slightly soluble in hydrocarbon solvents and fully soluble in aromatic and ethereal solvents. X−ray-quality single crystals were grown by slow diffusion from THF with pentane as the anti-solvent stored at −35 °C. Complex (**1**) displayed a six-coordinate distorted octahedral structure with a THF solvent molecule in the unit cell. The complex crystallized in the space group $P\bar{1}$. The structure shows that the acetylide is bound cis to N2 with a Li counterion situated between N1 and N2. The geometry of the complex differs greatly from the previously reported structure of yttrium benzyl complex, [K(THF)$_2$(NNN)YBn-(THF)$_2$], which featured π−cation interactions between the potassium countercation and the π system of the benzyl group.[12]

Scheme 1. Synthesis of (1) and Solid-State Structure of (1) Shown at 50% Thermal Ellipsoid Probability[a]

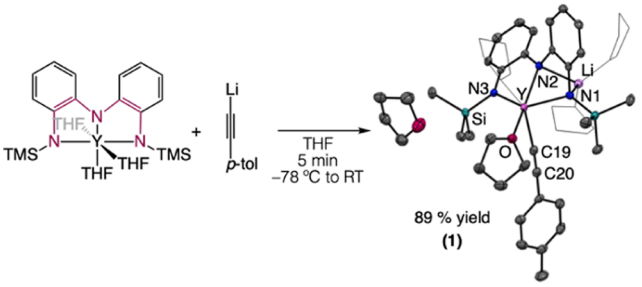

[a]Hydrogen atoms omitted for clarity. Colors: blue, N; red, O; teal, Si; pink, Y; purple, Li.

Synthesis and Characterization of Li(THF)$_3$(NNN)BH (2). The reactivity of (**1**) toward HB(pin) was investigated by adding HB(pin) to the acetylide complex at −78 °C (Figure 2a, **Route 1**). The resulting ^{11}B NMR spectrum displayed a mixture of two products. The major species was observed as a doublet at δ = 7.1 ppm, and the minor species was observed as a broad singlet at δ = 30.80 ppm in THF−d_8. This was interesting to us as our expected boron species would be neutral if transmetallation occurred. However, the shift of the major product's resonance was in the region where an anionic borate would appear. In the ^{1}H NMR spectrum, four aryl signals were observed, and the TMS groups displayed a single resonance at δ = 0.23 ppm, indicating that a symmetrical species was formed. Upon decoupling of the ^{11}B nucleus, the ^{1}H{^{11}B} NMR spectrum also displayed a broad singlet at δ = 4.25 ppm, which supports the presence of a B−H and is consistent with the doublet observed in the ^{11}B NMR. To confirm this unexpected result and elucidate the identity of our major species, X-ray-quality single crystals were grown from slow diffusion of THF with pentane as the anti-solvent stored at −35 °C. The Li(THF)$_3$(NNN)BH complex (**2**) crystallized in the space group $P22_1/n$. Complex (**2**) displayed a distorted tetrahedral geometry with the angle around N1−B−N3 being 118.74(19)° (Figure 2b). The Li counterion was situated in front of N2 at 2.107(5) Å. The hydride position was determined from an electron-density Fourier map. The bond length of the B−H bond was 1.18 Å, which is slightly longer than the expected value of 1.06 Å; however, attempts to restrain the bond length were unsuccessful. Separation attempts of (**2**) from the mixture of products were challenging; therefore, a different synthetic route was developed to characterize the complex. The second route to synthesize (**2**) involved deprotonation of the tris(amido) ligand, (NNN)H$_3$,

https://doi.org/10.1021/acs.organomet.5c00068
Organometallics 2025, 44, 995−999

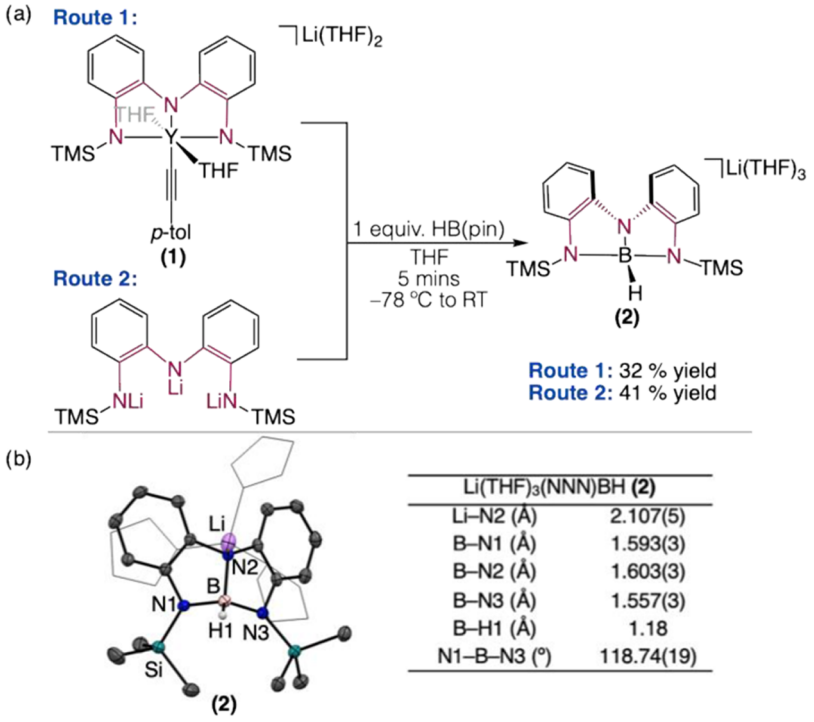

Li(THF)$_3$(NNN)BH (**2**)	
Li–N2 (Å)	2.107(5)
B–N1 (Å)	1.593(3)
B–N2 (Å)	1.603(3)
B–N3 (Å)	1.557(3)
B–H1 (Å)	1.18
N1–B–N3 (°)	118.74(19)

Figure 2. (a) Synthesis of (**2**). (b) Solid−state structure of (**2**) shown at 50% thermal ellipsoid probability and selected bond distances and angles for (**2**). Hydrogen atoms have been omitted for clarity except for B−H1. Colors: blue, N; red, O; teal, Si; light pink, B; purple, Li.

using a slight excess of *n*−BuLi at −78 °C and letting the reaction stir at room temperature for 2 h to form (NNN)Li$_3$, which was filtered and washed with pentane. HB(pin) was then added to (NNN)Li$_3$ to form (**2**) in 41% yield (Figure 2a, **Route 2**).

Synthesis and Characterization of (NNN)B (3). To further explore the identity of the minor product observed in the NMR spectrum of (**2**), we carried out its independent synthesis. Due to the symmetrical ^{1}H NMR spectrum, we hypothesized that the minor product is the tris(amido) ligand bound to boron, (NNN)B (**3**), where complete displacement of yttrium occurs. To test this hypothesis, trimethyl borate, B(OMe)$_3$, was added to (NNN)Y(THF)$_3$ complex in THF and stirred at room temperature for 24 h (Figure 3a). The reaction was filtered, and the ^{1}H NMR spectrum of this complex is consistent with the minor product. The ^{1}H NMR spectrum was symmetrical with one TMS resonance at δ = 0.51 ppm in THF−d$_8$. The ^{11}B NMR spectrum displayed a broad singlet at δ = 30.80 ppm. X−ray-quality single crystals were grown by slow evaporation from pentane with toluene as the anti-solvent stored at −35 °C. Complex (**3**) crystallized in the space group $P22_1/c$. The angles around the boron deviated slightly from that of ideal trigonal planar geometry, with the N1−B−N3 angle being 144.26 (10)° (Figure 3b). The ligand torsion angle θ, where θ = ∠C2−C3−C7−C12 across N2, is 8.28°. This is much smaller than the torsion angle observed for the rare earth metal complexes' counterparts.[12,14] The synthesis and computational electronic structure of boron complexes similar to (**3**) were previously reported by Martin et al. due to the unique geometry around boron; therefore, we wanted to explore the electrochemical properties of complex (**3**).[31] Additionally, electrochemical studies of the rare earth metal analogs of (**3**) have been reported, so we were interested in comparing their properties.[11−14] Cyclic voltammetry studies were conducted in 0.25 M [^{n}Bu$_4$N]PF$_6$ THF solutions with 3 mM of (**3**) at 100 mV/s under Ar and ambient temperature (Figure 3c). The cyclic voltammogram displayed one irreversible oxidation event at E_{pa} = 0.62 V vs FeCp$_2$. This is

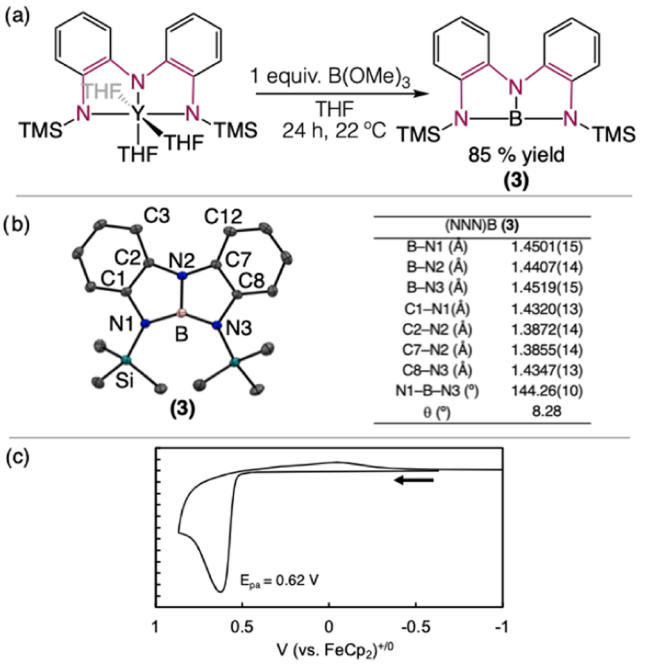

(NNN)B (**3**)	
B–N1 (Å)	1.4501(15)
B–N2 (Å)	1.4407(14)
B–N3 (Å)	1.4519(15)
C1–N1(Å)	1.4320(13)
C2–N2 (Å)	1.3872(14)
C7–N2 (Å)	1.3855(14)
C8–N3 (Å)	1.4347(13)
N1–B–N3 (°)	144.26(10)
θ (°)	8.28

Figure 3. (a) Synthesis of compound (**3**). (b) Solid-state structure of (**3**) shown at 50% thermal ellipsoid probability and selected bond distances and angles for (**3**). Hydrogen atoms are omitted for clarity. θ = ∠C2−C3−C7−C12 across N2. Colors: blue, N; red, O; teal, Si; light pink, B. (c) Cyclic voltammogram displaying the redox−processes for (**3**). CV was collected under Ar in 0.25 M [^{n}Bu$_4$N]PF$_6$ THF solution with 3 mM (**3**) at 100 mV/s at 298 K. Peak current potentials are normalized.

https://doi.org/10.1021/acs.organomet.5c00068
Organometallics 2025, 44, 995−999

a harsher oxidation potential when compared to the rare earth metal analogs (−0.82 to −1.03 V vs $FeCp_2$).[14] Moreover, the rare earth metal analogs displayed two separate oxidation events in their voltammograms. These differences in electrochemical properties suggest that (**3**) has unique reactivity, which should be explored.

Investigation of B−O Bond Cleavage Intermediate. Since (**1**) does not undergo transmetallation with HB(pin), we wanted to investigate the mechanism of B−O bond cleavage. Therefore, the reactivity of HB(pin) with the neutral (NNN)Y(THF)$_3$ complex was investigated (Figure 4a). The

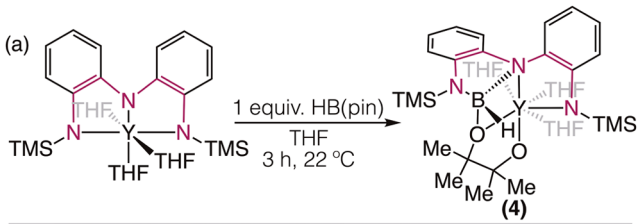

(b)

(NNN)Y(pinacolato)BH(THF)$_3$ (**4**)	
Y–N1 (Å)	2.315(3)
Y–N2 (Å)	2.491(3)
Y–B (Å)	3.041(4)
B–N2(Å)	1.611(5)
B–N3 (Å)	1.535(6)
B–O1 (Å)	1.515(5)
B–H1(Å)	1.13(5)
Y–O1(Å)	2.306(3)
Y–O2(Å)	2.112(3)
H1–B–O1 (°)	112(2)
O1–B–N3(°)	113.0(3)
N2–B–N3(°)	102.9(3)
N2–B–O1(°)	100.2(3)

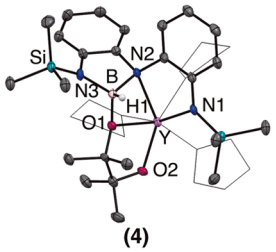

Figure 4. (a) Synthesis of (**4**). (b) Selected bond distances and angles for (**4**) and solid-state structure of (**4**) shown at 50% thermal ellipsoid probability. Hydrogen atoms omitted for clarity except for B−H1. Colors: blue, N; red, O; teal, Si; pink, Y; light pink, B.

reaction was monitored by ^{1}H NMR spectroscopy, where a minor amount of (**3**) was observed, as well as a new major product. Attempts to separate the two products were unsuccessful, as only broad signals were observed in the ^{1}H NMR spectrum after the addition of hydrocarbon solvents. To elucidate the identity of the major species, X−ray-quality single crystals were grown by slow evaporation from the reaction mixture in THF with toluene as the anti-solvent stored at −35 °C. The formation of (NNN)Y(pinacolato)BH(THF)$_3$ (**4**) was observed, which is seven coordinate around yttrium with pseudopentagonal bipyramidal geometry (Figure 4b). Complex (**4**) crystallized in space group *Pbcn*. Cleavage of the B−O bonds, where the pinacolato group is now bound to both the yttrium and boron atoms, was observed. The boron is still bound to the hydride, suggesting it might be an intermediate to forming (**2**). The hydride position was determined from the electron-density Fourier map. The B−H bond distance was 1.13(5) Å, which is shorter than the B−H bond length observed for (**2**). The ^{11}B NMR spectrum displays a broad signal at δ = 5.69 ppm in THF−d_8 and the geometry around the boron is pseudotetrahedral, which are both consistent with an anionic borate. Identifying the minor product as (**3**) allowed us to identify the ^{1}H NMR signals that correspond to the unsymmetrical (**4**), which had two TMS resonances at δ = 0.18 and 0.31 ppm and four B(pin) methyl resonances at δ = 0.90, 0.95, 1.22, and 1.48 ppm in THF−d_8. Given the structure of (**4**), it is likely that the loss of coordinating THF molecules destabilizes the complex and leads to decomposition, hence the difficulty in separation and isolation of (**4**).

To investigate whether complex (**4**) is an intermediate to the formation of (**2**), LiC$_2$*p*-tol was added to (**4**) in a 1:3 solvent mixture of C_6D_6/THF (Figure 5). This solvent mixture

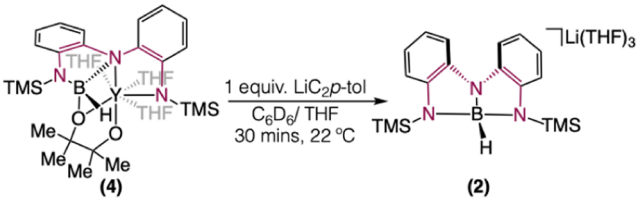

Figure 5. Reaction of (**4**) with LiC$_2$*p*-tol.

was used as it provided the cleanest reaction. The reaction was monitored by ^{1}H and ^{11}B NMR spectroscopy. Within 30 min of the reaction full conversion of (**4**) to (**2**) was observed, indicating that (**4**) is likely an intermediate to the formation of (**2**) (Figures S20−S22).

CONCLUSIONS

This work demonstrates the incompatibility of HB(pin) as a transmetallating reagent with yttrium complexes bearing a tris(amido) redox−active ligand. B−O bond cleavage is favored over B−H bond cleavage by these complexes, which results in side products that are deleterious to C−C cross−coupling. The B−O bond cleavage observed by these yttrium complexes likely results from a combination of the oxophilicity of yttrium and a better orbital overlap between the boron and nitrogen atoms resulting in more covalent bonds compared to the Y−N bond.[32] Future work on the reactivity of these newly formed boron complexes is underway. Furthermore, an investigation into how alkyl and aryl borane reagents behave with these early transition metal complexes is also in progress.

ASSOCIATED CONTENT

Supporting Information

The Supporting Information is available free of charge at https://pubs.acs.org/doi/10.1021/acs.organomet.5c00068.

Synthesis and characterization of complexes (**1**−**4**) (PDF)

Accession Codes

Deposition Numbers 2425044 and 2425046−2425048 contain the supplementary crystallographic data for this paper. These data can be obtained free of charge via the joint Cambridge Crystallographic Data Centre (CCDC) and Fachinformationszentrum Karlsruhe Access Structures service.

AUTHOR INFORMATION

Corresponding Author

Courtney C. Roberts − *Department of Chemistry, University of Minnesota, Minneapolis, Minnesota 55455, United States;* orcid.org/0000-0001-8177-4013; Email: ccrob@umn.edu

Author

Rana B. Abdu − *Department of Chemistry, University of Minnesota, Minneapolis, Minnesota 55455, United States;* orcid.org/0009-0003-5607-9539

https://doi.org/10.1021/acs.organomet.5c00068
Organometallics 2025, 44, 995−999

Complete contact information is available at:
https://pubs.acs.org/10.1021/acs.organomet.5c00068

Notes

The authors declare no competing financial interest.

■ ACKNOWLEDGMENTS

Financial support was provided in part by the NSF Award CHE-2237586. R.B.A. acknowledges the NSF-GRFP Award #2237827 and the Graham N. Gleysteen Departmental First Year Fellowship. C.C.R. acknowledges Amgen's Young Investigator Program, the McKnight Land-Grant professorship, and the 3M Alumni Professorship. X−ray diffraction experiments were performed using a crystal diffractometer acquired through an NSF−MRI award (CHE1229400) in the X−ray laboratory supervised by Dr. Victor G. Young. The authors would also like to acknowledge Alex Lovstedt for assistance with XRD collection and structure refinements and would also like to thank Nick A. Garcia for helpful discussions.

■ REFERENCES

(1) King, A. O.; Yasuda, N. Palladium-Catalyzed Cross-Coupling Reactions in the Synthesis of Pharmaceuticals. In *Organometallics in Process Chemistry*; Springer: Berlin, Heidelberg, 2004; pp 205−245.
(2) Devendar, P.; Qu, R.-Y.; Kang, W.-M.; He, B.; Yang, G.-F. Palladium-Catalyzed Cross-Coupling Reactions: A Powerful Tool for the Synthesis of Agrochemicals. *J. Agric. Food Chem.* **2018**, *66* (34), 8914−8934.
(3) Campeau, L.-C.; Hazari, N. Cross-Coupling and Related Reactions: Connecting Past Success to the Development of New Reactions for the Future. *Organometallics* **2019**, *38* (1), 3−35.
(4) Cassani, C.; Bergonzini, G.; Wallentin, C. J. Active Species and Mechanistic Pathways in Iron-Catalyzed C−C Bond-Forming Cross-Coupling Reactions. *ACS Catal.* **2016**, *6* (3), 1640−1648.
(5) Hedström, A.; Izakian, Z.; Vreto, I.; Wallentin, C.-J.; Norrby, P.-O. On the Radical Nature of Iron-Catalyzed Cross-Coupling Reactions. *Chem. - Eur. J.* **2015**, *21* (15), 5946−5953.
(6) Cahiez, G.; Moyeux, A. Cobalt-Catalyzed Cross-Coupling Reactions. *Chem. Rev.* **2010**, *110* (3), 1435−1462.
(7) Diccianni, J. B.; Diao, T. Mechanisms of Nickel-Catalyzed Cross-Coupling Reactions. *Trends Chem.* **2019**, *1* (9), 830−844.
(8) Thapa, S.; Shrestha, B.; Gurung, S. K.; Giri, R. Copper-Catalysed Cross-Coupling: An Untapped Potential. *Org. Biomol. Chem.* **2015**, *13* (17), 4816−4827.
(9) Nicolaou, K. C.; Bulger, P. G.; Sarlah, D. Palladium-Catalyzed Cross-Coupling Reactions in Total Synthesis. *Angew. Chem., Int. Ed.* **2005**, *44* (29), 4442−4489.
(10) Jana, R.; Pathak, T. P.; Sigman, M. S. Advances in Transition Metal (Pd, Ni, Fe)-Catalyzed Cross-Coupling Reactions Using Alkyl-Organometallics as Reaction Partners. *Chem. Rev.* **2011**, *111* (3), 1417−1492.
(11) Belli, R. G.; Tafuri, V. C.; Joannou, M. V.; Roberts, C. C. D0Metal-Catalyzed Alkyl−Alkyl Cross-Coupling Enabled by a Redox-Active Ligand. *ACS Catal.* **2022**, *12* (5), 3094−3099.
(12) Belli, R. G.; Tafuri, V. C.; Roberts, C. C. Improving Alkyl−Alkyl Cross-Coupling Catalysis with Early Transition Metals through Mechanistic Understanding and Metal Tuning. *ACS Catal.* **2022**, *12* (15), 9430−9436.
(13) Belli, R. G.; Tafuri, V. C.; Garcia, N. A.; Roberts, C. C. One- and Two-Electron Redox Catalysis with Lutetium Enabled by a Tris(Amido) Redox-Active Ligand. *Organometallics* **2023**, *42* (11), 1059−1064.
(14) Garcia, N. A.; Tafuri, V. C.; Abdu, R. B.; Roberts, C. C. Elucidating the Impact of Rare Earth or Transition Metal Identity on the Physical and Electronic Structural Properties of a Series of Redox-Active Tris(Amido) Complexes. *Inorg. Chem.* **2024**, *63* (33), 15283−15293.
(15) Giannerini, M.; Fañanás-Mastral, M.; Feringa, B. L. Direct Catalytic Cross-Coupling of Organolithium Compounds. *Nat. Chem.* **2013**, *5* (8), 667−672.
(16) Jia, Z.; Liu, Q.; Peng, X.-S.; Wong, H. N. C. Iron-Catalysed Cross-Coupling of Organolithium Compounds with Organic Halides. *Nat. Commun.* **2016**, *7* (1), No. 10614.
(17) Heijnen, D.; Tosi, F.; Vila, C.; Stuart, M. C. A.; Elsinga, P. H.; Szymanski, W.; Feringa, B. L. Oxygen Activated, Palladium Nanoparticle Catalyzed, Ultrafast Cross-Coupling of Organolithium Reagents. *Angew. Chem., Int. Ed.* **2017**, *56* (12), 3354−3359.
(18) Seyferth, D. The Grignard Reagents. *Organometallics* **2009**, *28* (6), 1598−1605.
(19) Nassar, Y.; Rodier, F.; Ferey, V.; Cossy, J. Cross-Coupling of Ketone Enolates with Grignard and Zinc Reagents with First-Row Transition Metal Catalysts. *ACS Catal.* **2021**, *11* (9), 5736−5761.
(20) Hoffmann, R. W.; Hölzer, B. Stereochemistry of the Transmetalation of Grignard Reagents to Copper (I) and Manganese (II). *J. Am. Chem. Soc.* **2002**, *124* (16), 4204−4205.
(21) Peltzer, R. M.; Gauss, J.; Eisenstein, O.; Cascella, M. The Grignard Reaction − Unraveling a Chemical Puzzle. *J. Am. Chem. Soc.* **2020**, *142* (6), 2984−2994.
(22) Dilman, A. D.; Levin, V. V. Advances in the Chemistry of Organozinc Reagents. *Tetrahedron Lett.* **2016**, *57* (36), 3986−3992.
(23) Rio, J.; Perrin, L.; Payard, P.-A. Structure−Reactivity Relationship of Organozinc and Organozincate Reagents: Key Elements towards Molecular Understanding. *Eur. J. Org. Chem.* **2022**, *2022* (44), No. e202200906.
(24) Cordovilla, C.; Bartolomé, C.; Martínez-Ilarduya, J. M.; Espinet, P. The Stille Reaction, 38 Years Later. *ACS Catal.* **2015**, *5* (5), 3040−3053.
(25) Suzuki, A. Organoborane Coupling Reactions (Suzuki Coupling). *Proc. Jpn. Acad., Ser. B* **2004**, *80* (8), 359−371.
(26) Suzuki, A. Cross-Coupling Reactions Of Organoboranes: An Easy Way To Construct C−C Bonds (Nobel Lecture). *Angew. Chem., Int. Ed.* **2011**, *50* (30), 6722−6737.
(27) Hartwig, J. The Mechanism of Cross−Coupling. In *Organotransition metal chemistry*; University Science Books, 2010; p 898.
(28) Wang, W.; Lv, Y.; Gou, X.; Leng, X.; Chen, Y. Boron-Oxygen Bond Cleavage of Pinacolborane and Catecholborane Mediated by a Scandium Phosphinidene Complex. *Chin. J. Chem.* **2014**, *32* (8), 752−756.
(29) Mao, W.; Xiang, L.; Lamsfus, C. A.; Maron, L.; Leng, X.; Chen, Y. Are Sc—C and Sc—P Bonds Reactive in Scandium Phosphinoalkylidene Complex? Insights on a Versatile Reactivity. *Chin. J. Chem.* **2018**, *36* (10), 904−908.
(30) Chu, J.; Wang, C.; Xiang, L.; Leng, X.; Chen, Y. Reactivity of Scandium Terminal Imido Complex toward Boranes: C(sp^3)−H Bond Borylation and B−O Bond Cleavage. *Organometallics* **2017**, *36* (23), 4620−4625.
(31) Huang, K.; Dutton, J. L.; Martin, C. D. Exploiting Pincer Ligands to Perturb the Geometry at Boron. *Chem. - Eur. J.* **2017**, *23* (44), 10532−10535.
(32) Kozuch, S. When, Where and Why Boron Prefers Boron to Nitrogen. *ChemPhysChem* **2024**, *25* (4), No. e202300875.